

Article

Molecular Dynamics Study of the Diffusion between Virgin and Aged Asphalt Binder

Yiqun Zhan , Hao Wu , Weimin Song * and Lin Zhu

School of Civil Engineering, Central South University, Changsha 410075, China; zhanyiqun@csu.edu.cn (Y.Z.); haoutk@csu.edu.cn (H.W.); 18681333982@163.com (L.Z.)

* Correspondence: wsong8@csu.edu.cn; Tel.: +86-180-7512-7569

Abstract: The diffusion between the virgin and aged asphalt binder in the recycled asphalt mixture is a crucial factor affecting its macro-mechanical performance. In this study, a combined model of the virgin-aged layered asphalt structure was assembled based on the molecular dynamics (MD) method. A four-component and twelve-category molecule were used to model the asphalt. The diffusion behaviors of the virgin and aged asphalt were characterized by mean square displacement (MSD), diffusion coefficient, relative concentration and cohesive energy density (CED). Results indicated that at the same temperature, the diffusion coefficient of the virgin asphalt was the largest, followed by the virgin-aged asphalt and the aged asphalt. As the temperature increased, the relative concentration on both sides of the virgin-aged asphalt overlapped to a certain extent. The covered lengths of the virgin asphalt were larger than those of the aged asphalt, indicating the diffusion between the virgin asphalt and aged asphalt was mainly manifested as the diffusion from the virgin asphalt to the aged asphalt. The development of CED and the fraction of free volume (FFV) indicated the mutual attractive interactions among the molecules in virgin and aged asphalt layers became strong and the cohesion properties inside the model became better.

Keywords: virgin-aged asphalt; molecular dynamics; mean square displacement; diffusion coefficient; relative concentration; cohesive energy density



Citation: Zhan, Y.; Wu, H.; Song, W.; Zhu, L. Molecular Dynamics Study of the Diffusion between Virgin and Aged Asphalt Binder. *Coatings* **2022**, *12*, 403. <https://doi.org/10.3390/coatings12030403>

Academic Editor: Andrea Nobili

Received: 23 February 2022

Accepted: 16 March 2022

Published: 18 March 2022

Publisher's Note: MDPI stays neutral with regard to jurisdictional claims in published maps and institutional affiliations.



Copyright: © 2022 by the authors. Licensee MDPI, Basel, Switzerland. This article is an open access article distributed under the terms and conditions of the Creative Commons Attribution (CC BY) license (<https://creativecommons.org/licenses/by/4.0/>).

1. Introduction

By the end of 2020, the total mileage of highways in China was up to 5.19 million kilometers [1], 99% of which needs different levels of maintenance. A large amount of reclaimed asphalt pavements (RAP) would be inevitably generated in pavement maintenance. If no reasonable measure was taken, lots of lands would be occupied. RAP may become a major pollution source to air and water. Therefore, the reuse of RAP in road engineering is a necessary way for current sustainable development. In road engineering, RAP could be used in subgrade or subbase. Due to the existence of a binder film coating on the aggregate, RAP could be used in the preparation of new asphalt mixtures, in which RAP could provide both binder and high-quality aggregate, thus reducing the demand for new raw materials, reducing the cost and preserving natural resources.

Blending occurs between the aged binder in RAP and virgin binder under the effect of high temperatures during mixing and compaction. The blending issue attracts extensive concerns around ensuring the quality of asphalt mixtures with RAP. The blending efficiency is an indicator characterizing the content and uniformity of mixing. The blending between the virgin and aged binder is a very complicated physicochemical process. Inadequate blending would induce various distresses, such as cracking and moisture damage. In studying the blending efficiency between the virgin and aged binder, the staged extraction method is commonly used nowadays [2–4]. Using the staged extraction method, it was found that only a small percentage of RAP binder blended with the virgin binder, while other parts acted as a stiff layer coating on RAP aggregates. However, the validity of the

stage extraction method is affected by many factors, such as washing time, temperature, solvent type, etc. [5]. Therefore, the adoption of the staged extraction method should be implemented with great caution. Some chemical techniques are generally used, combined with the staged extraction method, to understand the blending issue. Using Fourier Transform Infrared Spectroscopy (FTIR) and Gel Permeation Chromatography (GPC), Bowers et al., [2] found that the blending between the RAP binder and the virgin binder would occur in all layers of the RAP binder from the outside to the inside, although the blending was not uniform. Sreeram et al. [6] investigated the RAP binder mobilization and blending efficiency using the ATR-FRIR approach. Results indicated that the RAP mobilization was highly dependent on temperature; warm mix additives could help to increase the mobilization of RAP and its subsequent blending efficiency. Huang et al. [7] conducted FTIR and GPC tests to evaluate the effect of rejuvenators on bitumen's chemical and rheological characteristics. It was reported that the sulfoxide index of FTIR and three GPC parameters (weight-average molecular weight, polydispersity, and large molecular size) could be used as reliable indices to characterize the rheological properties of rejuvenated bitumen.

The chemical techniques provide tools to investigate the interaction between the virgin and aged asphalt and the effect of various additives on bitumen. However, these techniques could not give a clear insight into the molecular interactions. The microscopic behaviors from the perspective of the molecular can provide insights into a better understanding of the macroscopic performance [8–10]. With the rapid development of computer technology, molecular simulation methods have been commonly used in various fields. Molecular dynamics (MD) is a computational method to simulate the interactions and behaviors of multiple molecules and the related atoms under given conditions based on the fundamental principles of statistical mechanics and thermodynamics [11]. Generally, the trajectories of atoms and molecules were generated from Newton's equations of motion, where forces between particles and their potential energies are calculated using interatomic potentials or molecular mechanics force fields. The basic three elements of MD simulation can be concluded as force field, structure optimization and performance calculation. MD is a valuable tool to better understand the behaviors of asphalt and its mixtures from the microscopic perspective.

Asphalt is a major by-product extracted from crude oil. The components in asphalt are very complicated. A wealth of research shows that asphalt is composed of millions of different molecules [12–14], which present significant differences in physicochemical properties. To ensure the accuracy of MD simulations, the determination of the chemical composition and molecular structure is the first step. Zhang and Greenfield firstly regarded asphalt as a three-component mixture, including resin, saturate, and asphaltene [15]. Another component, aromatic, was introduced in the subsequent research [16–19]. With a deepening understanding of asphalt and the improvement at a computer level, more complicated asphalt models were generated, such as the 12-component asphalt molecular [20]. After establishing the asphalt model, the model accuracy is determined by verifying the parameters, such as density, viscosity, etc. Yao et al. used the Amber Cornell Extension Force Field to predict the physicochemical properties of asphalt [21]. The model contained three components: asphaltene, aromatic, and saturate. The density, viscosity and bulk modulus generated from MD modeling were close to the laboratory testing data.

Many researchers adopt the MD model of asphalt to simulate the mechanical properties of asphalt [10,22], the interaction between components [19], the diffusion behavior [16,23] and the effects of aging and modifiers on the asphalt behaviors [24]. The interfacial properties of asphalt/aggregate, including the mechanical effects of interfacial adhesion and moisture [25,26], were effectively predicted by MD simulation. Xu et al. developed a two-layered model to investigate the interaction between rejuvenator and RAP binder in the asphalt recycling process from the atomic scale [27]. Results showed that rejuvenator diffusion followed the Fickian equation. The rejuvenator could restore the thermodynamic properties and molecular structures to the virgin binder to a certain extent. Ding et al. investigated the diffusion between the virgin and aged asphalt binder [16]. Results indicated

that the diffusion was affected by both the diffusion ability itself and the properties of the diffusion acceptor. On the other hand, the order of adding a rejuvenator was a critical factor affecting the diffusion of the virgin and aged binders. Cui et al. investigated the effect of water, temperature, and the rejuvenator on the aged asphalt [24]. Results indicated that compared to improving the crack resistance, the effect of rejuvenators in aged asphalt on weakening the rutting resistance was more pronounced. Under high temperatures, a low dosage of rejuvenator presented higher diffusion coefficients than that of high dosage. Temperature and water showed coupled adverse effects on the work of adhesion between the asphalt and aggregate.

Besides, the self-healing capability of asphalt binder was also evaluated based on MD simulations [28,29]. The indices-diffusion coefficient, activation energy, and pre-exponential factor et al. were put forward to evaluate the self-healing performance. The effects of the molecule structure (chain length and branching), temperature and modifying agent (SBS) were explored. In summary, MD can effectively predict the performance of asphalt, and the macroscopic behaviors can be correlated to microscopic mechanisms. This technique is helpful to understand the various behaviors of asphalt from the microscopic perspectives, including the influencing factors of adhesion, cohesion, diffusion and engineering prediction, etc. Although [16] investigated the diffusion behaviors between the virgin and aged binders, the diffusion was explored from the point of each component. The MD model contained only three parts, including asphaltene, resin, and oil. In [18], the diffusion behaviors between the rejuvenator and the aged binder showed that naphthene aromatics performed best for diffusion, while polar aromatic performed the worst. In this study, authors investigated the diffusion between the virgin and aged binders using a more complicated model, and the investigation was conducted from the point of the whole model. The force field in this study was COMPASS (condensed-phase optimized molecular potentials for atomistic simulation studies), which was also different from [16,23]. This is the novelty of this study.

2. Objective and Scope

This study aimed to explore the diffusion behaviors between the virgin and aged asphalt. To make a comprehensive analysis, a two-layered molecular system was built up to simulate the diffusion under different temperatures. Densities of the virgin and aged asphalt were obtained firstly to verify the accuracy of the model. The mean square displacement (MSD), diffusion coefficient, relative concentration, and cohesive energy density (CED) were obtained during the diffusion process. The effect of temperature on these parameters was explored.

3. Model Building

3.1. Virgin Asphalt

Asphalt is complicated in composition and can be regarded as a three-component structure or a four-component structure. In 1993, Jennings et al. developed eight models for standardized asphalt samples studied in the SHRP plan [30]. Within the eight models, the AAA-1 model is most commonly used and has an almost equivalent chemical and mechanical performance to that of real asphalt. Therefore, based on the AAA-1 model, a numerical model describing the molecular structure of asphalt was established using a four-component and twelve-category molecular system, as shown in Figure 1. The compositions of the asphalt model can be seen in Table 1.

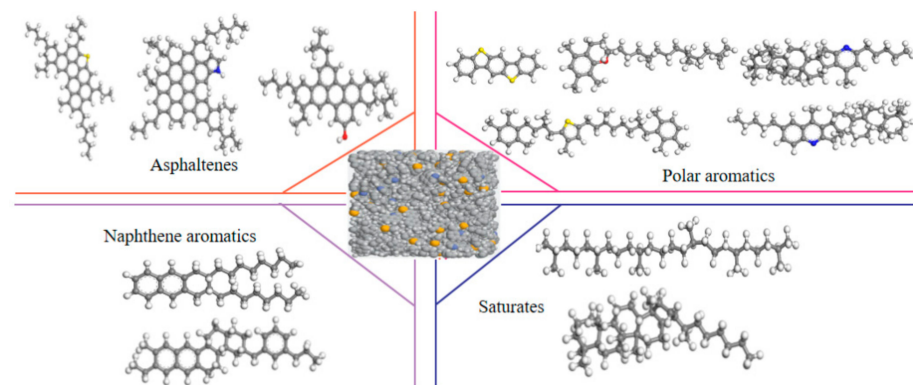


Figure 1. Molecular structure model of the virgin asphalt (carbon atoms are grey; hydrogen atoms are white; oxygen atoms are red; sulphur atoms are yellow; and the blue one is nitrogen).

Table 1. Compositions of the asphalt model.

Component	Number of Molecules	Chemical Formula	Proportion
Asphaltenes 1	3	C42H55O	17.3%
Asphaltenes 2	2	C66H81N	
Asphaltenes 3	3	C51H62S	
Naphthene aromatics 1	11	C35H44	31.9%
Naphthene aromatics 2	13	C30H46	
Saturates 1	4	C30H62	11.1%
Saturates 2	4	C35H62	
Polar aromatics 1	4	C40H59N	39.7%
Polar aromatics 2	4	C40H60S	
Polar aromatics 3	4	C36H57N	
Polar aromatics 4	5	C29H50O	
Polar aromatics 5	15	C18H10S2	

3.2. Aged Asphalt

The aging of asphalt generally has two stages: the first stage is early aging or rapid aging. In this stage, the asphalt material has a fast-aging rate, and sulfoxide is the major oxidation; the second stage is the long-term aging or continuous aging stage, in which the asphalt material has a relatively slow aging rate, and the changes in material properties caused by aging are fairly gentle. In this stage, the ketone group is the main oxidation product in the asphalt binder [31]. The ratio of sulfoxide group and ketone group during asphalt aging is related to oxygen concentration, sulfur content, temperature, and other factors. Some experimental investigations also revealed that the ketones and sulfoxides were major functional groups formed after oxidation [31,32]. Therefore, when building an aged asphalt model, ketone and sulfoxide groups can be introduced into the virgin asphalt model, where oxidation may occur to form an aged asphalt model. At the same time, as saturated phenols are long-chain alkanes, the properties of alkanes are relatively stable, and their oxidation can be ignored. In the aging asphalt model, the saturates consistent with the virgin asphalt model are still used.

In this study, the aged asphalt model and the component ratio of each group adopt the data in [33,34]. The components of the aged asphalt can be seen in Figure 2.

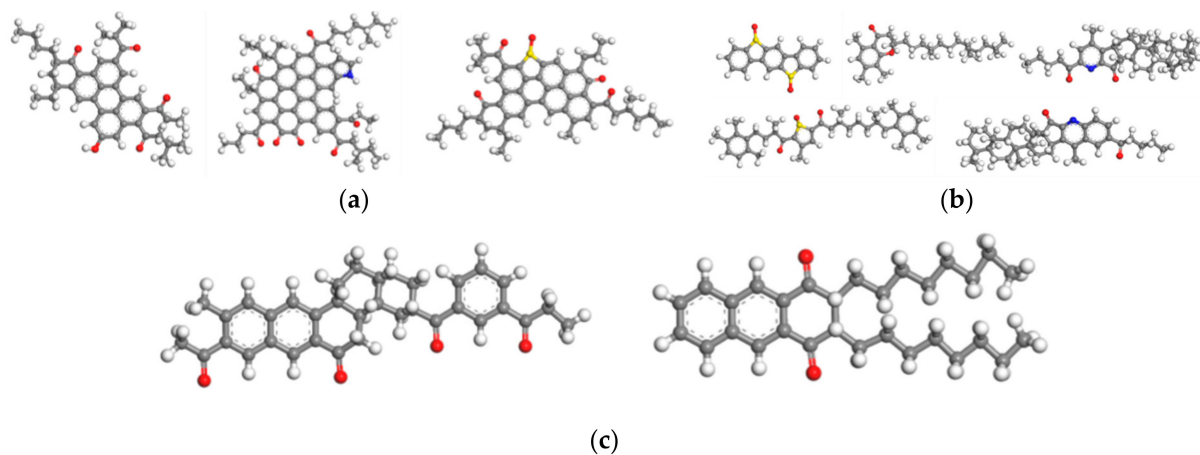


Figure 2. Molecular structure model of aged asphalt: (a) Asphaltenes; (b) Polar aromatics; (c) Naphthene aromatics (Oxygen atoms are red).

The COMPASS (condensed-phase optimized molecular potentials for atomistic simulation studies) field [35,36] was used in this study. It is the first ab initio forcefield that enables accurate and simultaneous prediction of structural, conformational, vibrational, and thermophysical properties for molecules in isolation and condensed phases. This force field has been validated to make accurate predictions of various material properties. The total energy can be calculated using Equation (1).

$$E_{\text{total}} = \sum E_b(b) + \sum E_\theta(\theta) + \sum E_\varphi(\varphi) + \sum E_{b,\theta,\varphi}(b,\theta,\varphi) + \sum E_\gamma(\gamma) + E_{\text{vdw}} + E_{\text{coulomb}} \quad (1)$$

where $\sum E_b(b)$ is the covalent bond stretching energy terms; $\sum E_\theta(\theta)$ is the bond angle bending energy terms; $\sum E_\varphi(\varphi)$ is the torsion angle rotation energy terms of the polymer chain; $\sum E_{b,\theta,\varphi}(b,\theta,\varphi)$ is cross interactions included in the dynamic variations among the bond stretching, bending, and torsion angle rotation; $\sum E_\gamma(\gamma)$ is the out-of-plane energy; E_{vdw} is the van der Waals force energy; E_{coulomb} is the Coulombic electrostatic force energy. $\sum E_b(b)$, $\sum E_\theta(\theta)$, $\sum E_\varphi(\varphi)$ and $\sum E_{b,\theta,\varphi}(b,\theta,\varphi)$ can be directly obtained when a model was set up. The out-of-plane interaction, also called inversion interaction, is part of nearly all forcefields for covalent systems. The van der Waals energy is obtained after optimization in a condensed system.

3.3. Layered Diffusion Model of the Virgin-Aged Asphalt

Under given temperatures, diffusion would occur between the virgin and aged asphalt binder. A constant pressure ensemble (NPT) was selected to simulate the diffusion process. As the temperature increased, the asphalt molecules on both sides of the simulated interface can flow freely, diffuse and gradually merge (Figure 3). The Nose–Hoover method was used to control the system temperature. The inherent rheological properties of asphalt are the main reason for the spontaneous molecular diffusion and randomization behavior, and this behavior requires appropriate temperature and time to stimulate. When a relatively high temperature or a long time is reached, the molecules move faster or penetrate each other more fully. Therefore, the nano-view interface would show higher fusion efficiency and a better fusion effect. In this study, three temperatures were selected, including 110 °C (383.15 K), 140 °C (413.15 K), and 170 °C (443.15 K). The temperature of 170 °C is generally slightly higher than the mixing temperature. The diffusion simulation at this temperature can investigate the effect of mixing on the diffusion between the virgin and aged asphalt. The temperature of 140 °C can be regarded as the temperature at which paving is conducted. When establishing the MD model, cell relaxation on the virgin asphalt and aged asphalt models was performed at three temperatures firstly; then, the layered virgin-aged asphalt model was built; lastly, the geometric optimization of the layered model was performed for 5000 iterations to obtain the final analysis model. Figure 3 is the layered diffusion model at 383.15 K.

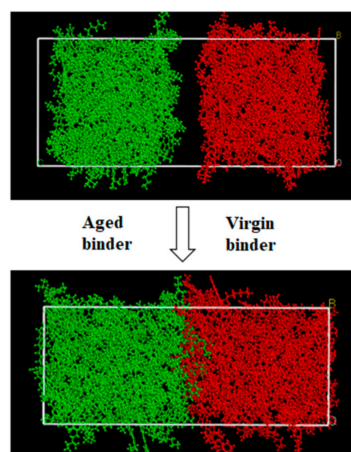


Figure 3. Molecular diffusion model of virgin and aged asphalt.

4. Results

4.1. Density Prediction

The virgin asphalt model and the aged asphalt model were developed firstly to calculate the densities. In the NPT ensemble at 300 K and 1 atm pressure, when the system was stable, the estimated densities were 0.984 and 1.055 g/cm³ for the virgin and aged asphalt, respectively, as shown in Table 2. The density of the aged asphalt was slightly higher than that of the virgin asphalt, which was due to the sulfoxide group and ketone group in the aged asphalt. The calculated density was consistent with the published data, indicating the model in this study is reasonable.

Table 2. Densities at 300 K.

Asphalt Type	Density (g/cm ³)	Published Data (g/cm ³)
Virgin asphalt	0.984	0.90–1.04 [37,38]
Aged asphalt	1.055	1.061 [27]

4.2. Mean Square Displacement (MSD) and Diffusion Coefficient

After establishing the virgin-aged asphalt layer model, some thermodynamic calculations were carried out to analyze the mutual diffusion behavior between the virgin and aged asphalt. MSD is the deviation of a particle's position towards a referenced position over time. It can be calculated using Equation (2).

$$MSD = \frac{1}{N} \sum_{n=1}^N [x_n(t) - x_n(0)]^2 \quad (2)$$

where N is the number of particles to be averaged, $x_n(0)$ is the referenced position of each particle and $x_n(t)$ is the specific position of a particle at time t .

The diffusion coefficient can be calculated using Equation (3).

$$D = \frac{1}{6N} \lim_{t \rightarrow \infty} \frac{d}{dt} \sum_{n=1}^N (x_n(t) - x_n(0))^2 \quad (3)$$

where $\frac{d}{dt}$ represents the slope of the MSD curve.

To explore the diffusion between the virgin and aged asphalt, we mainly studied the diffusion along the direction perpendicular to the interface, without considering the diffusion along with other directions. Due to the number of particles (N) being constant in the NPT ensemble, the slope of the curve between MSD and t is proportional to the diffusion coefficient. The greater the slope of the MSD curve, the greater the diffusion

coefficient, and the stronger the molecular diffusion ability. The diffusion coefficient can be obtained from the MSD curve, which is $1/6$ of the slope.

Figure 4 shows the diffusion between virgin and aged asphalt at 383.15 K. At 5 ps, the aged asphalt and virgin asphalt started to make contact, and the MSD was very large at this time. From 5 ps to 100 ps, the virgin and aged asphalt filled the original gap between the two layers. After 100 ps, the diffusion became stable. MD simulation under the NPT ensemble was conducted for 500 ps at each temperature.

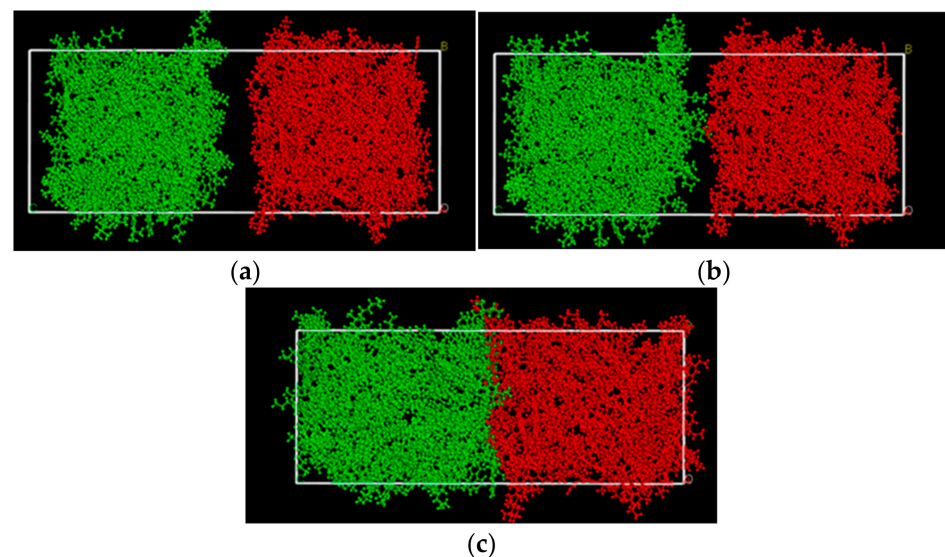


Figure 4. Diffusion between virgin and aged asphalt at 383.15 K: (a) $t = 0$; (b) $t = 5$ ps; (c) $t = 100$ ps.

MSDs of all the layers at different temperatures were plotted in Figure 5. It can be clearly observed that MSDs of the virgin asphalt were the largest, and the values of the aged asphalt were the lowest. Considering the entire asphalt model, the MSDs of the virgin-aged asphalt were between the values of the virgin and the aged asphalt. In these figures, linear fitting was conducted, and the slopes of the MSD curves can be derived. Thus, diffusion coefficients of all the layers were calculated and presented in Figure 6. It can be observed that no matter for the virgin asphalt, aged asphalt, or the entire model, the diffusion coefficient increased with the increasing temperature, which is consistent with our common sense. The diffusion coefficient of the aged asphalt layer was the smallest, while the diffusion coefficient of the virgin layer was the largest. This conclusion is consistent with previous findings [37,39]. Ding et al. also found that when the virgin asphalt and the aged asphalt diffused across the vacuum between them, the diffusion coefficient of the virgin binder was larger than that of the aged binder [40]. It was reported that after aging, the diffusion coefficients of all the four components in asphalt decreased, with the asphaltene and naphthene aromatic having the most considerable reduction [39]. Rad et al. prepared some samples of the two-layer binder, and adopted the Fick's law and DSR test to investigate the diffusion between the aged and virgin binder [41]. Results showed that the increase in temperature or conditioning time could lead to the increment of the diffusion coefficient.

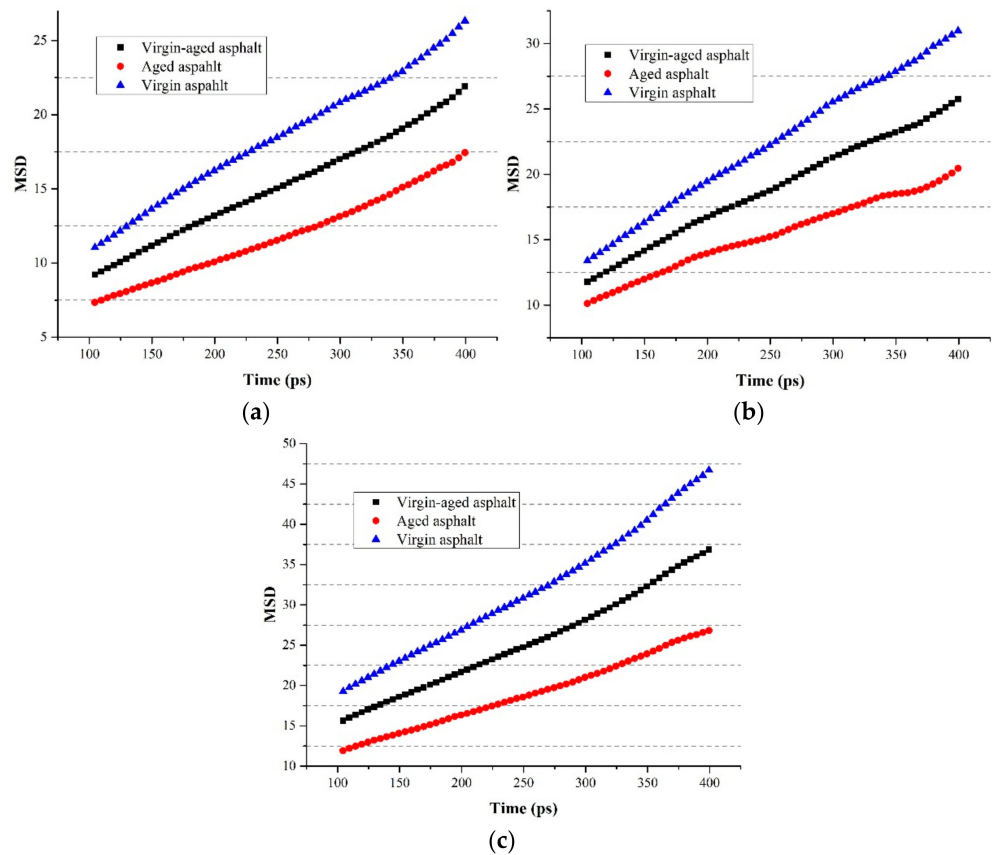


Figure 5. MSD at different temperatures: (a) 383.15 K; (b) 413.15 K; (c) 443.15 K.

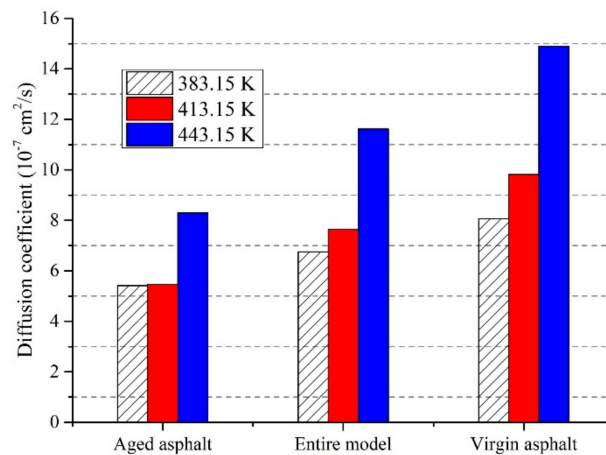


Figure 6. Diffusion coefficients at different layers.

4.3. Relative Concentration

In the mixing of hot mix asphalt (HMA) with RAP, due to the inconsistent content of components in the virgin and aged asphalt, there exists a difference in the substance concentration between the virgin and aged asphalt. The substances in the high-concentration area are affected by the concentration gradient and gradually diffuse to the low-concentration area. Due to the free movement of the molecular, the local density would be different in different positions of the diffusion space. Relative concentration is the proportion of the local density to the bulk density. When there is nothing molecular in a zone, the relative concentration is zero. If the substance has adequate diffusion in a zone, the density in

the zone is the same as the density of the entire system. The relative concentration can be calculated according to [42,43]

$$RC_i = \frac{C_i}{C_{bulk}} \quad (4)$$

$$C_i = \frac{N_i}{V_i} \quad (5)$$

where RC_i is the relative concentration of the slab i ; C_i is the concentration of the slab i ; C_{bulk} is the bulk concentration; N_i is the number of particles in the slab i ; V_i is the volume of the slab i .

Figure 7 shows the relative concentrations at different temperatures. Figure 7a shows the relative concentration at the initial state, in which an original gap existed between the virgin and aged binder. The cell length at this time was 100 Å. Figure 7b,c and d present the relative concentrations at 500 ps under the temperatures of 383.15, 413.15, and 443.15 K, respectively. It can be observed that the cell lengths at 383.15, 413.15 and 443.15 K were 89.31, 89.42, and 92.98 Å, which were lower than the cell length at the initial state. The overlapping lengths at 383.15, 413.15, and 443.15 K were 40~50, 37~50, and 37~50.5 Å, indicating that after 500 ps' simulation, significant diffusion existed, and a higher temperature could induce a larger overlap between the virgin and aged asphalt. It should be noted that at the two sides of the box, the virgin binder molecular could reach the boundary where the aged binder existed; the phenomenon was the same as the aged binder. This was ascribed to the fact that compared to other positions, the concentrations were lower at two sides; thus, molecular could easily reach the sides due to the low concentration gradients.

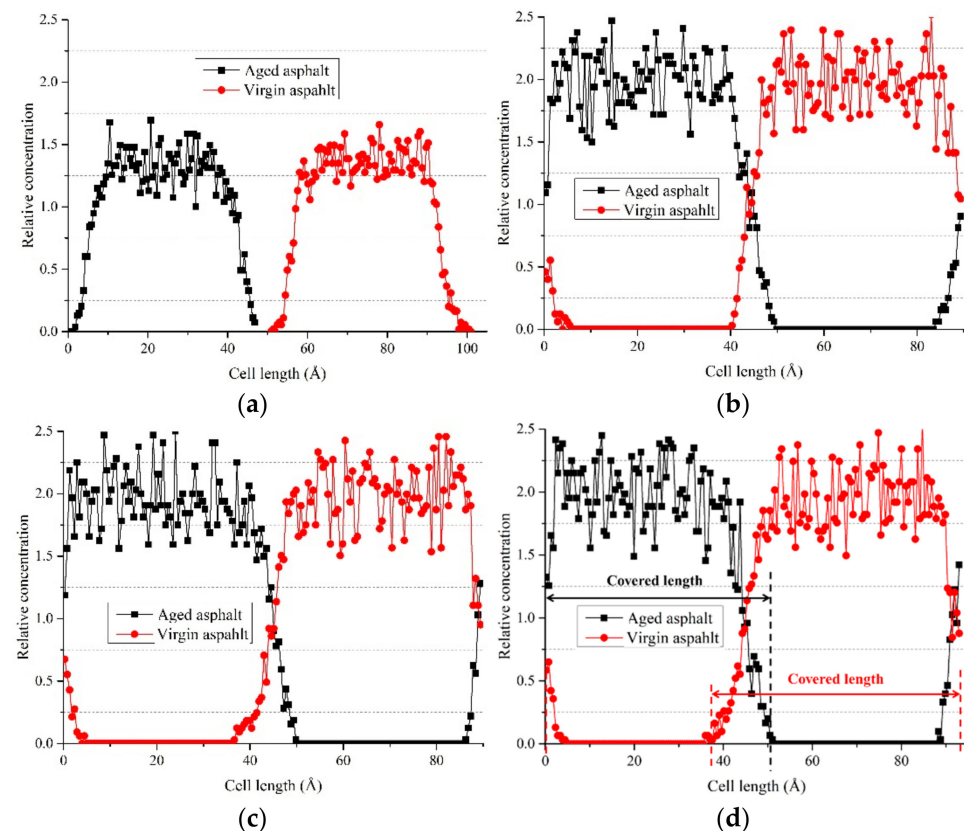


Figure 7. Relative concentration at different temperatures: (a) initial state; (b) 383.15 K; (c) 413.15 K; (d) 443.15 K.

To differentiate the diffusion efficiencies of the aged and virgin binder, it needs to detect the change of the covered lengths of the aged and virgin binder. The covered length is defined as the major length, in which the asphalt molecular covered, which can be seen

in Figure 7d. In Figure 8, the covered lengths of the virgin and aged asphalt were presented. It can be observed that the covered lengths of both the virgin and aged binder increased along with the increase in temperature, indicating temperature is a crucial factor affecting the diffusion. From 383.15 to 443.15 K, the covered length of the virgin asphalt increased by 14.6%, while the increase in the covered length of aged asphalt was 6.2%. This indicated that temperature promoted the diffusion of the virgin asphalt more obviously than it did to the aged asphalt. At the same temperature, the cover length of the virgin binder was larger than that of aged binder. Compared to the covered length of the aged binder, the covered length of the virgin binder increased by 0.77%, 6.4%, and 11.3% at 383.15 K, 413.15 K and 443.15 K, respectively. The diffusion between the virgin asphalt and aged asphalt was mainly manifested as the diffusion from the virgin asphalt to the aged asphalt.

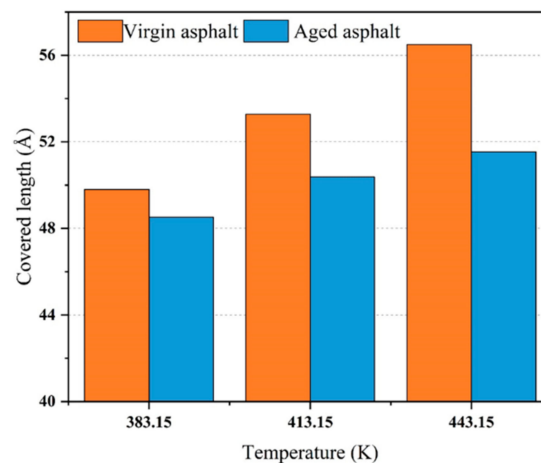


Figure 8. Covered lengths.

4.4. Cohesive Energy Density and Fraction of Free Volume

The cohesive energy density (*CED*) measures the mutual attractiveness of molecules to assess intermolecular interaction inside an asphalt molecular model. Asphalt with a higher *CED* value would possess superior cohesive strength. *CED* can be obtained from Equations (6) and (7).

$$E_{\text{coh}} = -\langle E_{\text{inter}} \rangle = \langle E_{\text{intra}} \rangle - \langle E_{\text{total}} \rangle \quad (6)$$

$$CED = \frac{E_{\text{coh}}}{V} \quad (7)$$

where E_{coh} is the cohesive energy, $\langle E_{\text{intra}} \rangle$ is the intermolecular energy in the model, $\langle E_{\text{total}} \rangle$ is the total energy in the system, V is the volume of the system.

The total volume (V) includes the free volume and the occupied volume. Free volume refers to the volume occupied by voids due to the irregular arrangement of molecular chains. The fraction of free volume (*FFV*) refers to the fraction of the free volume to the total volume. *FFV* can reflect the ability of the molecular chain to move freely to a certain extent. The lower the free volume of asphalt, the lower the molecular mobility, which would result in a phase transition from a viscoelastic state to a glass state [43].

$$FFV = \frac{V - V_O}{V} = \frac{V_F}{V} \quad (8)$$

where V_O is the occupied volume, V_F is the free volume.

CED and *FFV* reflect the macroscopic rheological properties and deformability of asphalt materials to a certain extent. In the actual mixing of HMA with RAP, it takes a certain amount of time for the virgin-aged asphalt to penetrate and diffuse each other. The degree of diffusion determines the performance of HMA with RAP. In this study, data of *CED* and *FFV* at 383.15 K for 500, 1000, 1500 and 2000 ps were derived and plotted in Figure 9. It can be observed that from 500 to 2000 ps, *CED* significantly increased, indicating

the mutual attractive interactions among the molecules in the virgin and aged asphalt layers became strong, and the cohesion properties inside the model became better. *FFV* decreased from 38.7% to 37.7%, indicating the interactions between the aged and virgin binder become stronger and the internal cohesion became more pronounced. The development trends of *FFV* and *CED* both indicated a better diffusion was induced with the increase in time. On the other hand, it was reported that the *CED* of asphalt is in the range of 3.19×10^8 to $3.22 \times 10^8 \text{ J}\cdot\text{m}^{-3}$, and the results of this study were generally consistent with [17].

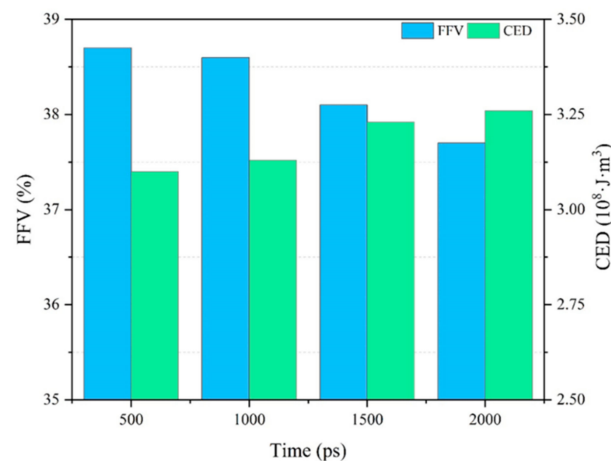


Figure 9. *FFV* and *CED* under different diffusion levels.

5. Conclusions

This study focused on evaluating the diffusion behaviors between virgin and aged asphalt. A two-layered model was set up to obtain various parameters to analyze the diffusion, including mean square displacement (MSD), diffusion coefficient, relative concentration, cohesive energy density, and the fraction of free volume. The results yielded the following conclusions:

- (1) The densities of the virgin and aged asphalt were consistent with the published data, indicating the four-component and twelve-category molecules can be used to model asphalt effectively.
- (2) No matter whether the virgin asphalt, aged asphalt, or the entire model, the diffusion coefficient increased with an increase in temperature. The diffusion coefficient of the aged asphalt layer was the smallest, while the diffusion coefficient of the virgin layer was the largest.
- (3) During the diffusion process, significant diffusion between the virgin and aged asphalt existed, and a higher temperature could induce a larger overlap length. At the same temperature, the covered lengths of the virgin binder were larger than those of the aged binder, indicating the diffusion between the virgin and aged asphalt was mainly manifested as the diffusion from the virgin asphalt to the aged asphalt.
- (4) During the diffusion, the fraction of free volume (*FFV*) gradually decreased from 38.7% to 37.7%, and the cohesive energy density (*CED*) increased from 3.10×10^8 to $3.26 \times 10^8 \text{ J}\cdot\text{m}^{-3}$, indicating as the mixing time increased, the interactions between the aged and virgin binder became stronger and the internal cohesion became more pronounced.

Author Contributions: Conceptualization, H.W. and W.S.; methodology, Y.Z. and L.Z.; software, L.Z.; validation, Y.Z. and L.Z.; formal analysis, Y.Z.; writing—original draft preparation, Y.Z.; writing—review and editing, W.S.; supervision, H.W.; funding acquisition, W.S. All authors have read and agreed to the published version of the manuscript.

Funding: This research was funded by National Natural Science Foundation of China (Grant Nos. 51778638 and 52008405).

Institutional Review Board Statement: Not applicable.

Informed Consent Statement: Not applicable.

Data Availability Statement: All data, models, and codes generated or used in this study are included in the submitted manuscript.

Conflicts of Interest: The authors declare no conflict of interest.

References

1. Gao, J.; Yang, J.; Yu, D.; Jiang, Y.; Ruan, K.G.; Tao, W.J. Reducing the variability of multi-source reclaimed asphalt pavement materials: A practice in China. *Constr. Build. Mater.* **2021**, *278*, 122389. [[CrossRef](#)]
2. Bowers, B.F.; Huang, B.S.; Shu, X. Investigation of Reclaimed Asphalt Pavement blending efficiency through GPC and FTIR. *J. Transp. Res. Board* **2014**, *50*, 517–523. [[CrossRef](#)]
3. Ding, Y.J.; Huang, B.S.; Hu, W.; Tang, B.M. Utilizing recycled asphalt shingle into pavement by extraction method. *J. Clean. Prod.* **2019**, *236*, 117656. [[CrossRef](#)]
4. Song, W.M.; Huang, B.S.; Shu, X. Influence of warm-mix asphalt technology and rejuvenator on performance of asphalt mixtures containing 50% reclaimed asphalt pavement. *J. Clean. Prod.* **2018**, *192*, 191–198. [[CrossRef](#)]
5. Zhao, S.; Huang, B.S.; Shu, X. Investigation on binder homogeneity of RAP/RAS mixtures through staged extraction. *Constr. Build. Mater.* **2015**, *82*, 184–191. [[CrossRef](#)]
6. Sreeram, A.; Leng, Z.; Zhang, Y.; Padhan, R.K. Evaluation of RAP binder mobilisation and blending efficiency in bituminous mixtures: An approach using ATR-FTIR and artificial aggregate. *Constr. Build. Mater.* **2018**, *179*, 245–253. [[CrossRef](#)]
7. Huang, W.D.; Guo, Y.F.; Zheng, Y.; Ding, Q.L. Chemical and rheological characteristics of rejuvenated bitumen with typical rejuvenators. *Constr. Build. Mater.* **2021**, *273*, 121525. [[CrossRef](#)]
8. Bazlamit, S.M.; Reza, F.J. Changes in Asphalt Pavement Friction Components and Adjustment of Skid Number for Temperature. *J. Transp. Eng.* **2005**, *131*, 470–476. [[CrossRef](#)]
9. Rashid, K.; Masoud, K.D.; Dallas, N.L.; Eyad, A.M. A micro-damage healing model that improves prediction of fatigue life in asphalt mixes. *Int. J. Eng. Sci.* **2010**, *48*, 966–990.
10. Fischer, H.R.; Cernescu, A.J.F. Relation of chemical composition to asphalt microstructure—Details and properties of microstructures in bitumen as seen by thermal and friction force microscopy and by scanning near-field optical microscopy. *J. Transp. Res. Board* **2015**, *153*, 628–633. [[CrossRef](#)]
11. Vlachakis, D.; Bencurova, E.; Papangelopoulos, N. Current state-of-the-art molecular dynamics methods and applications. *Adv. Protein Chem. Struct. Biol.* **2014**, *94*, 269–313. [[PubMed](#)]
12. Wiehe, I.A.; Liang, K.S.J.F.P.E. Asphaltenes, resins, and other petroleum macromolecules. *Energy Fuels* **1996**, *117*, 201–210. [[CrossRef](#)]
13. Rogel, E.; Carbognani, L.J.E. Density Estimation of Asphaltenes Using Molecular Dynamics Simulations. *Energy Fuels* **2003**, *17*, 378–386. [[CrossRef](#)]
14. Artok, L.; Su, Y.; Hirose, Y.; Hosokawa, M.; Murata, S.; Nomura, M. Structure and Reactivity of Petroleum-Derived Asphaltene. *Energy Fuels* **1999**, *13*, 287–296. [[CrossRef](#)]
15. Zhang, L.; Greenfield, M.L.J.E. Analyzing Properties of Model Asphalts Using Molecular Simulation. *Energy Fuels* **2007**, *21*, 1712–1716. [[CrossRef](#)]
16. Ding, Y.; Huang, B.S.; Shu, X.; Zhang, Y.Z.; Mark, E.W. Use of molecular dynamics to investigate diffusion between virgin and aged asphalt binders. *Fuel* **2016**, *174*, 267–273. [[CrossRef](#)]
17. Wang, L.B.; Lu, Y. Atomistic modelling of moisture sensitivity: A damage mechanisms study of asphalt concrete interfaces. *Road Mater. Pavement Des.* **2017**, *18*, 200–214.
18. Su, M.; Si, C.; Zhang, Z. Molecular dynamics study on influence of Nano-ZnO/SBS on physical properties and molecular structure of asphalt binder. *Fuel* **2020**, *263*, 116777. [[CrossRef](#)]
19. Wang, P.; Dong, Z.J.; Tan, Y.Q. Investigating the Interactions of the Saturate, Aromatic, Resin, and Asphaltene Four Fractions in Asphalt Binders by Molecular Simulations. *Fuel* **2015**, *29*, 150107113137004. [[CrossRef](#)]
20. Li, D.D.; Greenfield, M.L.J.F. Chemical compositions of improved model asphalt systems for molecular simulations. *Fuel* **2014**, *115*, 347–356. [[CrossRef](#)]
21. Yao, H.; Dai, Q.; You, Z. Molecular dynamics simulation of physicochemical properties of the asphalt model. *Fuel* **2016**, *164*, 83–93. [[CrossRef](#)]
22. Yao, H.; Dai, Q.; You, Z. Modulus simulation of asphalt binder models using Molecular Dynamics (MD) method. *Constr. Build. Mater.* **2018**, *162*, 430–441. [[CrossRef](#)]
23. Sun, W.; Wang, H. Molecular dynamics simulation of diffusion coefficients between different types of rejuvenator and aged asphalt binder. *Int. J. Pavement Eng.* **2020**, *21*, 966–976. [[CrossRef](#)]
24. Cui, B.Y.; Gu, X.G.; Hu, D.L.; Dong, Q. A multiphysics evaluation of the rejuvenator effects on aged asphalt using molecular dynamics simulations. *J. Clean. Prod.* **2020**, *259*, 120629. [[CrossRef](#)]

25. Sun, W.; Wang, H.J. Moisture effect on nanostructure and adhesion energy of asphalt on aggregate surface: A molecular dynamics study. *Appl. Surf. Sci.* **2020**, *510*, 145435. [[CrossRef](#)]
26. Wang, H.; Lin, E.; Xu, G. Molecular dynamics simulation of asphalt-aggregate interface adhesion strength with moisture effect. *Int. J. Pavement Eng.* **2017**, *18*, 414–423. [[CrossRef](#)]
27. Xu, G.; Wang, H.; Sun, W. Molecular dynamics study of rejuvenator effect on RAP binder: Diffusion behavior and molecular structure. *Constr. Build. Mater.* **2018**, *158*, 1046–1054. [[CrossRef](#)]
28. Bhasin, A.; Bommavaram, R.; Greenfield, M.L. Use of Molecular Dynamics to Investigate Self-Healing Mechanisms in Asphalt Binders. *J. Mater. Civ. Eng.* **2011**, *23*, 485–492. [[CrossRef](#)]
29. Sun, D.L.; Lin, T.; Zhu, X. Indices for self-healing performance assessments based on molecular dynamics simulation of asphalt binders. *Comput. Mater. Sci.* **2016**, *114*, 86–93. [[CrossRef](#)]
30. Jennings, P.W.; Pribanic, J.A.; Franconi, B. *Binder Characterization and Evaluation by Nuclear Magnetic Resonance Spectroscopy*; Strategic Highway Research Program: Washington, DC, USA, 1993.
31. Petersen, J.C.; Harnsberger, P. Asphalt aging: Dual oxidation mechanism and its interrelationships with asphalt composition and oxidative age hardening. *Road Mater. Pavement Des.* **1998**, *1638*, 47–55. [[CrossRef](#)]
32. Petersen, J.C.; Glaser, R. Asphalt Oxidation Mechanisms and the Role of Oxidation Products on Age Hardening Revisited. *Transp. Res. Rec.* **2011**, *12*, 795–819. [[CrossRef](#)]
33. Zhou, X.X.; Zhao, G.Y.; Wu, S.P. Effects of biochar on the chemical changes and phase separation of bio-asphalt under different aging conditions. *J. Clean. Prod.* **2020**, *263*, 121532. [[CrossRef](#)]
34. Xu, G.; Hao, W. Molecular dynamics study of oxidative aging effect on asphalt binder properties. *Fuel* **2017**, *188*, 1–10. [[CrossRef](#)]
35. Sun, H.; Ren, P.; Fried, J.R. The COMPASS force field: Parameterization and validation for phosphazenes. *Comput. Theor. Polym. Sci.* **1998**, *8*, 229–246. [[CrossRef](#)]
36. Sun, H. COMPASS: An ab Initio Force-Field Optimized for Condensed-Phase Applications—Overview with Details on Alkane and Benzene Compounds. *J. Phys. Chem. B* **1998**, *102*, 7338–7364. [[CrossRef](#)]
37. Gomez-Meijide, B.; Ajam, H.; Lastra-Gonzalez, P. Effect of ageing and RAP content on the induction healing properties of asphalt mixtures. *Constr. Build. Mater.* **2018**, *179*, 468–476. [[CrossRef](#)]
38. Zhang, X.; Ning, Y.; Zhou, X. Quantifying the rejuvenation effects of soybean-oil on aged asphalt-binder using molecular dynamics simulations. *J. Clean. Prod.* **2021**, *317*, 128375. [[CrossRef](#)]
39. He, L.; Li, G.N.; Lv, S.T.; Gao, J. Self-healing behavior of asphalt system based on molecular dynamics simulation. *Constr. Build. Mater.* **2020**, *254*, 119225. [[CrossRef](#)]
40. Farhad, Y.; Nima, R.S.; Bahia, H. Application of Diffusion Mechanism: Degree of Blending Between Fresh and Recycled Asphalt Pavement Binder in Dynamic Shear Rheometer. *Transp. Res. Rec.* **2014**, *2444*, 71–77.
41. Liu, J.; Yu, B.; Hong, Q. Molecular dynamics simulation of distribution and adhesion of asphalt components on steel slag. *Constr. Build. Mater.* **2020**, *255*, 119332. [[CrossRef](#)]
42. Long, Z.; You, L.; Tang, X. Analysis of interfacial adhesion properties of nano-silica modified asphalt mixtures using molecular dynamics simulation. *Constr. Build. Mater.* **2020**, *255*, 119354. [[CrossRef](#)]
43. Ren, S.; Liu, X.; Zhang, Y. Multi-scale characterization of lignin modified bitumen using experimental and molecular dynamics simulation methods. *Constr. Build. Mater.* **2021**, *287*, 123058. [[CrossRef](#)]